JCTC Journal of Chemical Theory and Computation

$HO_2 + O_3$ Reaction: Ab Initio Study and Implications in Atmospheric Chemistry

Luís P. Viegas and António J. C. Varandas*

Departamento de Química, Universidade de Coimbra, 3004-535 Coimbra, Portugal

Received July 17, 2009

Abstract: We report a theoretical investigation on the reaction between ozone and the hydroperoxyl radical, which is part of the ozone depletion cycle. This reaction represents a great challenge to the state of the art ab initio methods, while its mechanism remains unclear to both experimentalists and theoreticians. In this work we calculated the relative energies of the stationary points along the reaction coordinate of the oxygen- and hydrogen-abstraction mechanisms using different levels of theory and extrapolating some of the results to the complete one-electron basis set limit. Oxygen abstraction is shown to be preceded by formation of hydrogen-bonded complexes, while hydrogen abstraction shows a lower energy barrier than oxygen abstraction. Both mechanisms lead to formation of $HO_3 + O_2$ in a very troublesome region of the potential-energy surface that is not correctly described by single-reference methods. The implications of the results on reaction dynamics are discussed.

1. Introduction

The reaction of hydroperoxyl radical with ozone is the rate-limiting step in the natural cycle for ozone depletion:[1]

$$HO_2 + O_3 \xrightarrow{k_1} OH + 2O_2 \quad (1)$$

$$HO + O_3 \xrightarrow{k_2} HO_2 + O_2 \quad (2)$$

$$\text{net: } 2O_3 \rightarrow 3O_2 \quad (3)$$

This process is mostly active in the lower stratosphere over much of the globe, and it is believed to be responsible for approximately one-half of the global ozone loss in this atmospheric layer.[2] Knowledge of k_1 is therefore of crucial importance in order to calculate ozone profiles in the stratosphere and to make reliable modeling of atmospheric ozone phenomena.[3−6]

Not surprisingly, the title reaction became much studied experimentally over the years so as to determine k_1 and unravel the mechanistic details of eq 1.[7−15] An intriguing aspect of the title reaction is the positive curvature at low temperatures reported for the Arrhenius plot $\ln k_1(T)$ vs T^{-1}. Such a curvature is often due to competition of different reaction channels, which led Sinha et al.[11] and Nelson and Zahniser[13] to carry out a mechanistic study of reaction 1 using isotopic labeling of the oxygen atoms. Their sophisticated experimental work suggests that the title reaction proceeds via two distinct mechanisms:

$$H^{18}O_2 + {}^{16}O_3 \rightarrow {}^{18}OH + {}^{18}O^{16}O + {}^{16}O_2 \quad (4)$$

$$\rightarrow {}^{16}OH + {}^{18}O^{18}O + {}^{16}O_2 \quad (5)$$

Thus, in mechanism 4 ^{18}OH production occurs via oxygen abstraction from ozone, whereas ^{16}OH formation in eq 5 would imply ozone hydrogen abstraction. In order to decide about the two mechanisms, Nelson and Zahniser[13] measured the $^{16}OH/^{18}OH$ product branching ratio over the temperature range $226 \leq T/\mathrm{K} \leq 355$. The results have shown that both ^{16}OH and ^{18}OH are formed, with their analysis suggesting that hydrogen abstraction by ozone accounts for 88% of the reactive encounters, with this fraction increasing with decreasing temperature to ~95% at 226 K. Such an observation supports an earlier estimate of (75 ± 10)% by Sinha et al.[11] Nelson and Zahniser[13] further concluded that "the barrier to oxygen abstraction by ozone exceeds that for hydrogen abstraction by 1 ± 0.4 kcal mol^{-1}".

* Corresponding author phone/fax: +351-239-835867; e-mail: varandas@qtvs1.qui.uc.pt.

10.1021/ct900370q
Published on Web 01/22/2010

In spite of the relative abundance of experimental work, theoretical studies of reaction 1 are rather scarce in the literature. In fact, only three papers have been published so far concerning the study of $HO_2 + O_3$ on theoretical grounds.[16−18] The first one, by Varandas and Zhang,[16] presented a dynamics study of the title reaction using a test potential-energy surface (PES) for ground-state $HO_5(^2A)$ based on the double many-body expansion (DMBE) method.[19−21] In this work, they showed that the saddle-point structure representing ozone being attacked by HO_2 from the O end obtained from the HO_5 DMBE-4B (DMBE PES ignoring $n \geq 5$ terms) was similar to the structure obtained by performing exploratory complete active space self-consistent field (CASSCF) calculations considering 11 electrons and 11 active molecular orbitals and employing a 6-311G(2df) one-electron basis set, briefly CASSCF(11,11)/6-311G(2df). A six-body term was then added to the DMBE-4B PES so that the dynamics calculations would reproduce within error bars the recommended value of the rate constant for reaction 1 at room temperature. From these calculations, the authors predicted reaction 1 to occur almost exclusively via oxygen abstraction. This contrasts with the conclusions extracted from isotopically labeled experiments,[11,13] and they tentatively attributed this discrepancy to the presence of fast isotopic scrambling reactions (which are supposed to be absent from the mentioned experimental work), namely

$$^{18}OH(v) + {}^{16}O_3 \rightarrow H^{18}O^{16}O + {}^{16}O_2 \qquad (6)$$

where ^{18}OH is vibrationally excited. More recently, two theoretical studies on the title reaction have been reported. One of them, by Mansergas and Anglada,[17] focuses on the gas-phase hydrogen-bonded species (these and other intermediates will be hereinafter referred to as complexes) formed between HO_2 and O_3. The authors account for six stationary points, all energetically below the separated reactants: three minima interconnected by three saddle points. These stationary points were calculated by performing geometry optimizations at the CASSCF(m, n)/6-311+G(2df,2p) level of theory (CASSCF(19,15) and CASSCF(15,13) for the minimum structures and CASSCF(11,10) for the saddle points). The reported minima and one of the saddle points were further optimized with the QCISD approach[22] using the same basis set, while the stability of such stationary points was calculated by performing single-point energy calculations at the geometries predicted at the CCSD(T)/aug-cc-pVTZ level of theory. This was considered by the authors as their best level of theoretical treatment and can be indicated by CCSD(T)/aug-cc-pVTZ//QCISD/6-311+G(2df,2p). These energies were then subtracted from the energies of the reactants calculated with the same level of theory and with basis set superposition error (BSSE) corrections according to the counterpoise method of Boys and Bernardi.[23] The hydrogen-bonded complexes were found do be stable by no more than $\sim$3.7 kcal mol^{-1} and are suspected to be formed in the early stages of the mechanism of reaction 1 as a prereactive complex. For a review on the importance of the formation of radical−molecule complexes, see ref 24 and references therein. The latest study on the $HO_2 + O_3$ reaction is from Xu and Lin,[18] where the authors investigate the mechanism and kinetics of the title reaction. The geometries of the stationary points were optimized at the spin-unrestricted BH&HLYP/6-311++G(2df,2p) level of theory, while the relative energies were obtained with the G2M(CC2) method.[25] Two saddle points energetically above the reactants were reported: the first corresponds to the barrier to oxygen abstraction and has a similar structure to the one previously reported by Varandas and Zhang;[16] the second represents the barrier to hydrogen abstraction, which is reported by the authors to be 1 kcal mol^{-1} below the former saddle point. This energy difference was found to be consistent with the one suggested in previous experimental work.[11,13]

In this work we performed a theoretical study of the title reaction, analyzing both its oxygen- and hydrogen-abstraction mechanisms. Such a task was performed by carefully mapping, connecting, and calculating the relative energies of the relevant stationary points of the $HO_5(^2A)$ PES. This theoretical work is part of an ongoing study that intends to clarify the mechanistic details of the $HO_2 + O_3$ reaction and to improve the DMBE $HO_5(^2A)$ PES[16] for future dynamics studies. The next two sections present the theory and computational methods used in this work and the results and discussion, respectively. They are both divided in the same way for an easy understanding and correspondence between the problematics addressed in each subsection. The last section presents the conclusions and a brief discussion about future work in the title system.

2. Theory and Computational Methods

The theoretical study of the title reaction consisted of two main steps: (1) finding the first-order saddle points of the oxygen- and hydrogen-abstraction mechanisms and performing intrinsic reaction coordinate (IRC) calculations in order to identify which minima they connect; (2) calculating the relative energies between the stationary points obtained in the previous step. Each of these steps carries its own difficulties and will be addressed separately. All calculations have been performed in the ground state of $HO_5(^2A)$ with the GAMESS[26] and molpro[27] packages. The MacMolPlt[28] graphical user interface was used for visualization of the geometric and electronic features of the different stationary points.

2.1. Geometry Optimizations. The choice of an electronic structure method applied to the mapping of a PES, especially in reaction pathways where one is looking for first-order saddle points, must be made with great care. At such geometries, often associated with bond breaking, it is natural to encounter wave functions with an increasing degree of multireference character. At such regions of the PES, the use of single-reference methods is often problematic. On the other hand, the use of a multireference approach may require expertise and be computationally expensive. Thus, one needs some pragmatism in choosing a method capable of being flexible to correctly describe the PES regions of interest while being computationally affordable.

In this study, all geometry optimizations and IRC calculations have been done with the CASSCF method, which we believe to be the method that best fits the requirements stated

above. Following previous work,[16] the orbital space consists of 15 core orbitals, 11 active orbitals, and 11 active electrons. This active space has been chosen with the automatic procedure of Pulay and Hamilton,[29] who suggested that the unrestricted Hartree−Fock (UHF) natural orbitals can be used as a good starting point for the CASSCF calculations. The active space should then contain the fractionally occupied UHF natural orbitals, which in this work have been defined as the ones with occupation numbers between 1.998 and 0.002. Additionally, with the goal of getting more accurate geometries, we improved the basis set used before:[16] p-type polarization functions have been added to the hydrogen atom while diffuse functions were added to both the hydrogen and oxygen atoms. The geometry optimizations have then been carried out at the CASSCF(11,11)/6-311++G(2df,2p) level of theory without imposing constraints. The nature of each stationary point has been examined via analysis of the harmonic vibrational frequencies.

2.2. Relative Energies. The calculation of the relative energies of the stationary points of $HO_5(^2A)$ is a delicate subject. Generally speaking, at some regions of the PES, the wave function may have a high degree of single-reference nature while at regions of bond forming or breaking the wave function can be expected to have some degree of multireference character. In this case, one requires to account for both the dynamical and the nondynamical electron correlation effects. For small systems, the MRCI or even FCI approaches can be used to accurately map out the entire PES, but for larger systems, such as the one presented in this work, those methods can be prohibitive. One possibility is to use multireference perturbation theory (MRPT), although this method may not be free from problems.[30−32] The difficulties imposed by the title system and the lack of sufficient related theoretical work in the literature lead us to test and analyze several ab initio methods in the study of reaction 1. The different methods have all been utilized as implemented in the molpro[27] package for electronic structure calculations: CASSCF,[33−37] CASPT2,[38−41] CCSD,[42−44] and CCSD(T),[45,46] with the single-reference methods using the restricted open-shell Hartree−Fock (ROHF) method. We further employed density functional theory (DFT) in the study of such a reaction. As for choosing the BH&HLYP functional, two reasons may be advanced: first, the same functional has been utilized in previous work,[18] and hence, the published results can offer data for comparison; second, some preliminary tests have shown that the BH&HLYP functional yields accurate results. The BH&HLYP calculations have been carried out with the GAMESS[26] package.

The augmented correlated-consistent polarized valence X-tuple zeta (aug-cc-pVXZ or simply AVXZ) and the augmented correlated-consistent polarized core−valence X-tuple zeta (aug-cc-pCVXZ or ACVXZ) basis sets,[47−49] with $X = D, T, Q$ have been employed in all single-point energy calculations. Built in a manner that is intended to relate the correlation energy to the cardinal number X in a systematic way, such basis sets have prompted the search for laws to extrapolate the correlation energy to the complete one-electron basis set (CBS) limit[50−54] at $X = \infty$.

In this work, we applied the CBS extrapolation procedure to the coupled-cluster energies. For this, the electronic energy is first split as

$$E_X = E_X^{\mathrm{HF}} + E_X^{\mathrm{cor}} \tag{7}$$

To treat the uncorrelated Hartree−Fock energies, the two-point extrapolation formula recommended by Karton and Martin[55] has been utilized. For the AV(T, Q)Z pair, it assumes the form

$$E_X^{\mathrm{HF}} = E_\infty^{\mathrm{HF}} + B/X^{5.34} \tag{8}$$

In turn, the correlation energy employed the newly developed uniform singlet-pair and triplet-pair extrapolation (USTE) method,[56] which can be cast into the form

$$E_X^{\mathrm{cor}} = E_\infty^{\mathrm{cor}} + A_3 Y \tag{9}$$

with Y being defined by

$$Y = (X + \alpha)^{-3}\left[1 + \frac{A_5}{A_3}(X + \alpha)^{-2}\right] \tag{10}$$

Equation 9 is also a two-point extrapolation formula with parameters E_∞^{cor} and A_3. The numerical values of the parameters in eq 10 are dependent on the ab initio method and can be obtained by consulting Table 1 of ref 56.

The energetics of the stationary points have been referred to the reactants of the oxygen-abstraction reaction (**R$_O$**), $HO_2 + O_3$, which has been assumed as a supermolecule where the fragments are separated by 150 Å.

3. Results and Discussion

3.1. Geometry Optimizations. The calculated stationary points for the oxygen-abstraction mechanism can be seen in Figure 1.

We started our calculations by optimizing **SP$_1$**. The geometry of the saddle point is in almost perfect agreement with the one found before,[16] the only relevant difference being the three dihedral angles which are now slightly bigger in absolute value (maximum difference is ∼14°). The O−O forming bond is predicted to be 1.935 Å, 0.231 Å larger than the one reported by Xu and Lin.[18] The associated imaginary frequency is 557i cm^{-1}, and IRC calculations in the direction of the reactants show that this saddle point is linked to a minimum structure which we refer as **MIN$_1$**, corresponding to the structure **C1** reported by Mansergas and Anglada.[17] The distance from the hydrogen atom to the nearest oxygen from ozone in **MIN$_1$** is 2.404 Å, in excellent agreement with the value of 2.393 Å reported for **C1**, obtained at the CASSCF(19,15)/6-311+G(2df,2p) level of theory. A similar structure is obtained by Xu and Lin[18] (**LM1**), with the O−H distance being somewhat different, namely, 2.195 Å. However, these authors report **LM1** as a minimum that is connected to the hydrogen-abstraction saddle point. According to Mansergas and Anglada,[17] the two isomers of **C1** are linked by a saddle point (**TS1**), and indeed, we have confirmed this by obtaining the **SP$_2$** saddle point and running IRC calculations. The calculated imaginary

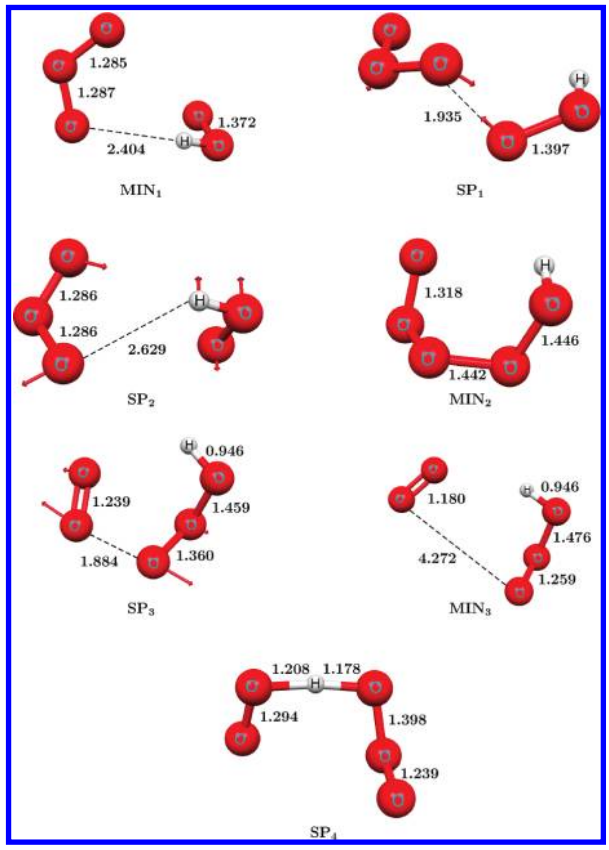

Figure 1. Geometries of the stationary points of the oxygen- and hydrogen-abstraction mechanisms for the title reaction. The calculations were performed on the HO_5 doublet state PES and optimized at the CASSCF(11,11)/6-311++G(2df,2p) level of theory. The arrows show the vector displacements associated to the corresponding imaginary frequencies, except for **SP_4**, which has the associated vector displacements hidden by the representation of the bonds between H and O. Distances are in Angstroms.

frequency is 42i cm^{-1}, and its geometry is very similar to the **TS1** structure, with a distance of 2.629 Å between the hydrogen atom and both terminal oxygen atoms of ozone. However, despite the fact that the calculations are well converged (calculations at DFT/BH&HLYP level carried out in the present work also predict a saddle point but with a frequency of 75 cm^{-1}), the low frequency of **SP_2** indicates that the PES is rather flat; thus, the possibility that it is artificial cannot be entirely ruled out. Such a **SP_2** structure resembles the one encountered for ground-state HO_3[57,58] and HO_4[59,60] before the complexes break to form products. The minimum **MIN_1** is therefore linked to both **SP_1** and **SP_2** saddle points (in the eventuality of **SP_2** being in fact a saddle point), which is a novel though somewhat questionable result as far as this mechanism is concerned. The details can be seen in Scheme 1. By following the vector displacements associated with the imaginary frequency of **SP_1** through IRC calculations, we conclude that this saddle point is linked to another minimum of the PES, **MIN_2**, where a bond of 1.442 Å is now formed between one of the terminal atoms of ozone and the hydroperoxyl radical. This is a significant difference from the results of Xu and Lin,[18] since they do not find a minimum structure resulting from their oxygen-abstraction process. Instead, they obtain $HO_3 + O_2$ which is known[57,61−63] to easily fragment to $HO + 2O_2$. Our calculations show that **MIN_2** is connected to the **SP_3** saddle point, which represents the energy barrier to overcome so that reaction can proceed to $HO_3 + O_2$. This saddle point has an imaginary frequency of 333i cm^{-1}, while the breaking O−O bond distance is 1.884 Å. Only then the reaction path proceeds to a minimum structure (**MIN_3**) where O_2 and HO_3 are well separated, with the O−O bond distance being 4.272 Å.

The calculated stationary points for the hydrogen-abstraction mechanism are represented at the bottom of Figure 1. As in the previous case, we started the calculations by optimizing the first-order saddle point, **SP_4**, which now represents the attack of the hydroperoxyl radical to the ozone molecule from the H end. The optimized geometry shows similarities to the one found by Xu and Lin,[18] for example, the hydrogen atom is separated from the two closest oxygen atoms by 1.208 and 1.178 Å, while Xu and Lin[18] predict 1.063 and 1.356 Å, respectively. The imaginary frequency of this saddle point is 4227i cm^{-1}, as indicated in Table 1, together with the remaining imaginary frequencies calculated in this work and in the previous theoretical studies of $HO_5(^2A)$. The different imaginary frequencies of **SP_4** deserve a comment. Although this work and ref 18 refer to the same type of motion of the hydrogen atom (switching between the O_2 and the O_3 fragments), the directional characteristics of the atoms are different as the norms of the direction vectors of almost all oxygen atoms in ref 18 are bigger than the ones here reported. In **SP_4**, practically only the two oxygen atoms closest to the hydrogen atom are displaced in the vibrational motion, making the imaginary frequency obtained in the present work resemble more the one of "pure" OH stretching in the diatomic, thus with a larger (imaginary) value.

Note that all frequencies have been calculated without scaling, which is known to generally lower the ab initio frequencies, bringing them to a closer agreement with the experimental counterparts. In the particular case of the CASSCF calculations in HO_5, an increase in the active space would also lower the frequencies, especially the one associated with the OH stretching.[17]

The IRC path in the products direction calculated in the present study is in close agreement with previous work.[18] The calculations show that **SP_4** is also connected to **MIN_3**, which is similar to **LM2** obtained by Xu and Lin[18] (see Figure 1 for more details). However, the IRC results from the present work disagree in the backward direction as they show that, when distorting away from the saddle point, the ozone and hydroperoxyl radical fragments break away without forming any kind of complex, while in ref 18 it yields the **LM1** complex mentioned previously. In summary, both the oxygen- and hydrogen-abstraction mechanisms share the fact that at some point of the reaction coordinate the O_2 molecule separates from the HO_3 fragment. Because of this and the fact that the minimum energy path of the oxygen-abstraction mechanism of the $HO_5(^2A)$ DMBE PES[16] shows a similar behavior, the optimizations have been terminated at this stage of the reaction coordinate. It should be stressed that the emphasis has been on the **SP_1** and **SP_4** saddle points

Scheme 1. Schematic Diagram Showing the Energetics of the Title Reaction[a]

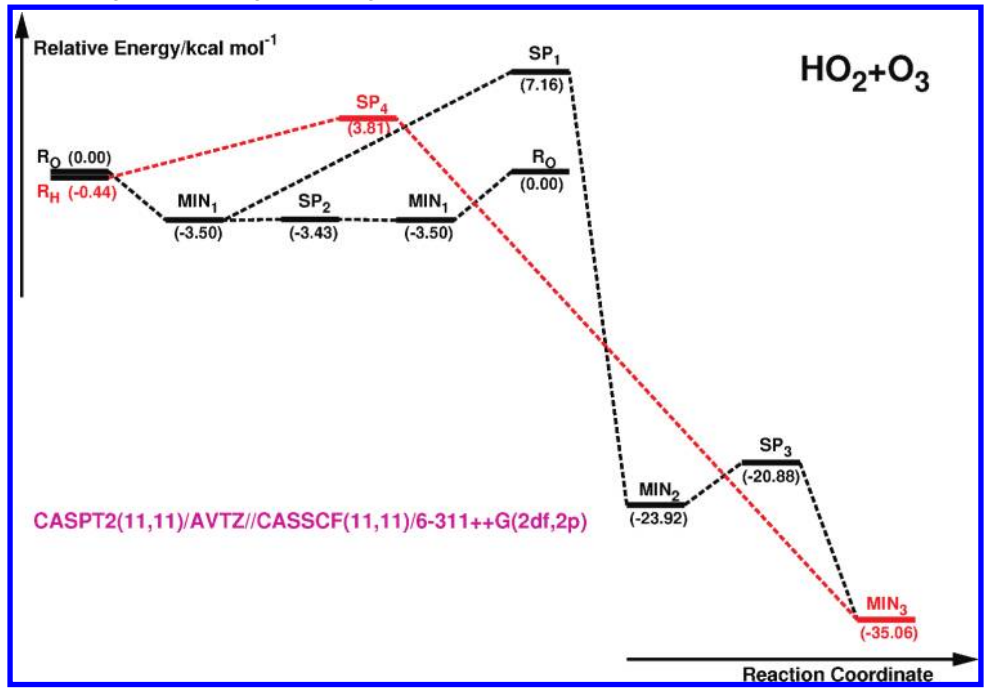

[a] The energies (in kcal mol^{-1}) are relative to the reactants of the oxygen-abstraction mechanism calculated at the CASPT2(11,11)/AV*TZ*//CASSCF(11,11)/6-311++G(2df,2p) level. The red lines connect the structures belonging to the hydrogen-abstraction mechanism, while the black lines do the same for the oxygen-abstraction mechanism.

Table 1. Comparison between the Imaginary Frequencies, in cm^{-1}, of All Saddle Points Obtained in This Work and the Ones Obtained in Previous Theoretical Studies

	ref 16	ref 17	ref 18	this work
SP$_1$	573[a]		630[b]/741[c]	557
SP$_2$		117[d]		42
SP$_3$				333
SP$_4$			2089[b]/2927[c]	4227

[a] CASSCF(11,11)/6-311G(2df). [b] BH&HLYP/6-311++G(2df,2p). [c] MP2/6-311++G(2df,2p). [d] CASSCF(11,10)/6-311+G(2df,2p).

Table 2. Electronic Energies, in kcal mol^{-1}, of the Different Stationary Points Relative to the Reactants (R_O) at Different Levels of Theory

method	**MIN$_1$**	**SP$_1$**	**SP$_2$**	**MIN$_2$**	**SP$_3$**	**MIN$_3$**
CASSCF(11,11)/AV*TZ*	–1.48	11.28	–1.46	8.24	16.77	–6.81
CASPT2(11,11)/AV*TZ*	–3.50	7.16	–3.43	–23.92	–20.88	–35.06
CCSD/AV*TZ*	–3.40	15.30	–3.37	–11.22	12.24	–10.38
CCSD/ACV*TZ*	–3.32	15.66	–3.30	–11.13	–3.94	–10.86
CCSD(T)/AV*TZ*	–3.74	11.97	–3.73	–5.53	17.60	–1.58
CCSD(T)/ACV*TZ*	–3.66	12.22	–3.66	–5.41	–15.36	–1.93
BH&HLYP/AV*TZ*	–2.51	15.26	–2.41	–16.90	–10.90	–15.81

with a view to improve the $HO_5(^2A)$ DMBE PES,[16] since they play a key role in dynamics calculations.

3.2. Relative Energies. We begin our analysis by addressing the first part of the oxygen-abstraction mechanism, in which the formation of the hydrogen-bonded complexes takes part. By inspecting Table 2 we can see that all calculations place **SP$_2$** above **MIN$_1$**, except the CCSD(T)/ACV*TZ* one, which places the two stationary points at the same height. The stability of **MIN$_1$** is in good agreement with the best level of theoretical treatment reported by Mansergas and Anglada[17] for **C1**, −3.68 kcal mol^{-1}, and in reasonable agreement with the results of Xu and Lin[18] for

Table 3. Electronic Energies, in kcal mol^{-1}, of Selected Stationary Points Relative to the Reactants (R_O) with the CCSD and CCSD(T) Methods Using the AV*XZ* Basis Sets[a]

method	**MIN$_1$**	**SP$_2$**	**MIN$_2$**	ΔE^{iso}
CCSD/AV*DZ*	–3.70	–3.71	–9.47	–0.01
CCSD/AV*TZ*	–3.40	–3.37	–11.22	0.03
CCSD/CBS	–3.23	–3.18	–11.11	0.05
CCSD(T)/AV*DZ*	–4.06	–4.09	–4.27	–0.03
CCSD(T)/AV*TZ*	–3.74	–3.73	–5.53	0.01
CCSD(T)/CBS	–3.56	–3.53	–5.09	0.03

[a] In the CBS calculation, the Hartree–Fock value was extrapolated from the (*T*, *Q*) pair and the correlation energy was extrapolated from the (*D*, *T*) pair, i.e., $E_\infty = E_\infty^{HF}(T, Q) + \mathrm{USTE}(D, T)$. ΔE^{iso} is the barrier of isomerization, E (SP$_2$) – E(MIN$_1$).

LM1, −2.5 kcal mol^{-1}. The CASSCF results deviate the most from the ones obtained with the other methods, but this is to be expected, since a CASSCF calculation lacks dynamical correlation. Inspection of the CI coefficients of the CASSCF wave function of the reactants, **MIN$_1$** and **SP$_2$** also indicates that they mainly have single-reference character, and therefore, the use of an ab initio method that only promotes excitations from the Hartree−Fock determinant is, in principle, a good approximation. This is also the case with **MIN$_2$**, where the single-reference character of the CASSCF wave function is even higher than the previous cases. The USTE extrapolation method was then used along with the CCSD and CCSD(T) ab initio methods to obtain more accurate energies for these stationary points and also with the purpose of benchmarking this method. Note that the extrapolation to the CBS limit should also minimize the BSSE.[64] The results can be seen in Tables 3 and 4. The isomerization barrier, ΔE^{iso}, increases as the CBS limit is reached and never surpasses 0.05 kcal mol^{-1}. Note that all coupled-cluster calculations employing double-ζ basis sets

Table 4. Electronic Energies, in kcal mol^{-1}, of Selected Stationary Points Relative to the Reactants (R_O) with the CCSD and CCSD(T) Methods Using the ACV*XZ* Basis Sets[a]

method	**MIN$_1$**	**SP$_2$**	**MIN$_2$**	ΔE^{iso}
CCSD/ACV*DZ*	–3.79	–3.80	–9.87	–0.01
CCSD/ACV*TZ*	–3.32	–3.30	–11.13	0.02
CCSD/CBS	–3.07	–3.03	–10.79	0.04
CCSD(T)/ACV*DZ*	–4.15	–4.18	–4.68	–0.03
CCSD(T)/ACV*TZ*	–3.66	–3.66	–5.41	0.00
CCSD(T)/CBS	–3.39	–3.38	–4.70	0.01

[a] In the CBS calculation, the Hartree–Fock value was extrapolated from the (*T*, *Q*) pair and the correlation energy was extrapolated from the (*D*, *T*) pair, i.e., $E_\infty = E_\infty^{HF}(T, Q)$ + USTE-(*D*, *T*). ΔE^{iso} is the barrier of isomerization, E (SP$_2$) – E(MIN$_1$).

place **SP$_2$** slightly below **MIN$_1$**, which is reflected on the negative sign of ΔE^{iso}, indicating their possible inadequacy in this rather flat region of the PES. The CBS results for ΔE^{iso} are in close agreement with the ones obtained with CASSCF and CASPT2 using the AV*TZ* basis set: 0.02 and 0.07 kcal mol^{-1}, respectively. The BH&HLYP results place **MIN$_1$** and **SP$_2$** approximately 1 kcal mol^{-1} above the other calculations, coinciding with **LM1**,[18] having $\Delta E^{iso} = 0.1$ kcal mol^{-1}. It should be emphasized that the small value of ΔE^{iso} in conjunction with the low imaginary frequency of **SP$_2$** casts doubt on the true existence of this stationary point. All of our ΔE^{iso} results are below the ones obtained by Mansergas and Anglada,[17] 1.26 or 1.33 kcal mol^{-1}, depending on the active space used for the geometry optimization of the hydrogen-bonded minimum. However, besides using a different basis set and active space for the geometry optimizations, they also use a different level of theory for the single-point energy calculations of this barrier: CASPT2(19,15)/6-311+G(2df,2p).

The second part of this mechanism comprises the attack of the hydroperoxyl radical to the ozone molecule from the O end, which is represented by **SP$_1$**. The weight of the Hartree−Fock determinant on the wave function decreases to 65% at this geometry as indicated by the square of the corresponding coefficient in the determinantal expansion of the CI wave function. The coupled-cluster and DFT energies are at least about 4 kcal mol^{-1} above the CASPT2 energies, the latter being considered the most accurate energies for this point as they include the effect of the several determinants with considerable weight in the electronic wave function. The multireference character of **SP$_1$** can also be seen in the significant increase of the number and value of the t_2 cluster amplitudes for this stationary point. The CCSD and CCSD(T) results for **MIN$_2$** seem surprising at first, especially because at the Hartree−Fock level this point is 22.61 kcal mol^{-1} below the reactants. This result is in very good agreement with the CASPT2 calculation, leading us to think that there is some kind of problem in the balance between the coupled-cluster energies of the reactants and **MIN$_2$**. To better understand these coupled-cluster energies, we investigated the T_1 and D_1 diagnostics[65−67] of the reactants, **MIN$_1$**, **SP$_2$**, and **MIN$_2$**, results which are presented in Table 5. For both basis sets, the T_1 diagnostics are identical between the four geometries, the same happening for the D_1 diagnostics, with the exception of **MIN$_2$**, which has a higher

Table 5. T_1 and D_1 Diagnostics Obtained After CCSD Calculations of Selected Geometries with the AV*TZ* and ACV*TZ* Basis Sets

	AV*TZ*			ACV*TZ*		
geometry	T_1	D_1	T_1/D_1	T_1	D_1	T_1/D_1
R$_O$	0.0325	0.1257	0.2584	0.0280	0.1237	0.2261
MIN$_1$	0.0330	0.1283	0.2573	0.0284	0.1262	0.2250
SP$_2$	0.0330	0.1283	0.2571	0.0284	0.1262	0.2248
MIN$_2$	0.0325	0.1370	0.2370	0.0278	0.1347	0.2065

D_1 value. This has consequences in the T_1/D_1 ratio, which becomes smaller for **MIN$_2$**. According to Lee,[67] a value of T_1/D_1 which is much smaller than $1/\sqrt{2}$ "indicates that there is a large variation in orbital rotation parameters in the coupled-cluster wave function, or in other words, there are problem areas in the molecule and other areas where the coupled-cluster approach is performing better." Clearly, one finds two sets of ratios for both basis sets: the first set involves the reactants, **MIN$_1$** and **SP$_2$**, and the second set is composed only of **MIN$_2$**. This explains the excellent results obtained for the relative energies of **MIN$_1$** and **SP$_2$** with CCSD, since they are the result of performing differences between geometries belonging to the first set, where a favorable cancellation of errors occurs. The same does not hold for the relative energy of **MIN$_2$**, because it involves a difference between absolute energies of the two sets, where the T_1/D_1 ratio of **MIN$_2$** indicates more problem areas in this geometry. This unbalance in the coupled-cluster wave functions of the two sets leads to an increase of the relative energy of this point. This behavior is most likely a consequence of calculating the energy in a geometry optimized with a completely different electronic structure method. In fact, we observe that calculations carried out on a minimum geometry optimized with B3LYP rather than CASSCF yield energies of −17.80 and −24.32 kcal mol^{-1}, respectively, for CCSD and CCSD(T); cf. Table 2. In this case, the T_1/D_1 ratio increases, which is an indication that there are less problem areas in this new geometry. A similar problem occurs in the calculation of the perturbative corrections of connected triple excitations as it is known that the presence of large singles amplitudes can cause instability in this method. Again, it just so happens that the reactants, **MIN$_1$** and **SP$_2$**, have the same number of t_1 amplitudes above 0.05 with almost equal absolute values, contrasting with the **MIN$_2$** calculation which shows a large number of larger magnitude. The result is that the relative energy of **MIN$_2$** at the CCSD(T) level gets even higher because of this unbalanced treatment, and as already mentioned, the calculation of the relative energies of **MIN$_1$** and **SP$_2$** benefits from a cancellation of errors. The computation of coupled-cluster energies including quadruply excited clusters would help to clarify the extent of these considerations. Note that, as expected, Tables 3 and 4 show that the coupled-cluster calculations correlating all the orbitals with the ACV*XZ* basis set do not alter the results significantly.

The last two geometries obtained in this reaction coordinate are the **SP$_3$** and **MIN$_3$** stationary points, having less than 5% of single-reference character. The coupled-cluster results are thus completely untrustworthy. The BH&HLYP

Table 6. Comparison between the Energies of the Common Stationary Points Calculated in This Work and in Ref 18[a]

	R_H	MIN_1	SP_1	SP_4	MIN_3
CASPT2(11,11)/AV*TZ*	–0.44	–3.50	7.16	3.81	–35.06
BH&HLYP/AV*TZ*	–4.00	–2.51	15.26	14.25	–15.81
ref 18 [G2M(CC2) method]	0.00	–2.50	5.00	4.00	–36.40

[a] Energy units are in kcal mol^{-1}.

calculations are the only ones that can compete with the CASPT2 level of theory, but even in this case the results are still far away from the quality obtained with MRPT. The same reasoning holds for **SP$_4$**, which is part of the hydrogen-abstraction mechanism. Table 6 shows a comparison between the energies of the common stationary points calculated in this work and in ref 18.

Note that the CASPT2 dissociation energy of the reactants in the hydrogen-abstraction mechanism (**R$_H$**) is 0.44 kcal mol^{-1} below its counterpart in the oxygen-abstraction mechanism (**R$_O$**). Such a difference may be explained by the dissimilarity of the geometries of the fragments in each dissociation channel as a result of the different mechanisms involved and the fact that the products are not infinitely separated in practice. This difference rises to 4 kcal mol^{-1} at the BH&HLYP level. Another important result is the confirmation of the lower energy of **SP$_4$** with respect to **SP$_1$** both in absolute as in relative terms. This means that there are effectively two competitive reaction channels, and their influence in the dynamics of reaction 1 should be investigated in the future. The G2M(CC2) energies used in ref 18 show an interesting agreement with the CASPT2 method, although it seems rather surprising that such an agreement occurs due to the strong multireference character of several stationary points.

It should be mentioned that new generations of the single-reference coupled-cluster methods are available[68−70] that can handle significant degrees of multireference character quite well while offering a high-level description of dynamical correlations. In fact, we tested one of the so-called completely renormalized coupled-cluster methods, CR-CC(2,3), for some geometries (**R$_O$**, **MIN$_1$**, **MIN$_2$**, **SP$_1$**, **SP$_2$**) with the AV*DZ* basis set (the calculations employing V*TZ* or AV*TZ* basis sets are computationally too demanding), but no significantly different results have been found. For other geometries, which show a high degree of multireference character, we often had trouble in converging the lambda vector iterations.

4. Conclusions and Future Work

In this study, the oxygen- and hydrogen-abstraction mechanisms of the $HO_2 + O_3$ reaction have been computationally investigated with the CASSCF, CASPT2, CCSD, CCSD(T), and BH&HLYP theoretical methods. The optimizations were performed at the CASSCF(11,11)/6-311++G(2df,2p) level of theory, while the energetics of the title reaction was investigated with the previously mentioned methods.

Of the several saddle points located, two represent the attack of the hydroperoxyl radical to ozone from the O and H end. They are **SP$_1$** and **SP$_4$**, respectively. Some stationary points of both mechanisms (**SP$_3$**, **SP$_4$**, **MIN$_3$**, and, to a smaller extent, **SP$_1$**) have a high degree of multireference character, leading to the expected failure of the single-reference methods used in this work, CCSD and CCSD(T). The best level of theoretical treatment is therefore assumed to be CASPT2. Conversely, the first part of the oxygen-abstraction mechanism, where the formation of the hydrogen-bonded complexes takes place, is mainly single-reference in nature. The agreement between all the ab initio methods in this region of the PES is therefore expected, with the exception of **MIN$_2$**, for the reasons explained before. The connection of this part of the mechanism to the formation of **SP$_1$** is a novel result with possible implications in the reactions dynamics, since the energy barrier to the formation of **SP$_1$** is increased by a considerable amount and the barrier is likely to get narrower. The presence of the hydrogen-abstraction barrier, **SP$_4$**, is also expected to have an impact on the dynamics, namely, lowering the value of k_1. This does not necessarily mean that a stronger agreement between theoretical and experimental interpretations will be observed, because of two main reasons. First, the open-chain structure of **MIN$_2$** suggests the possibility that OH will be formed vibrationally excited, therefore increasing k_2 from a factor of ∼25 times[71,72] the value used by experimentalists to analyze their data. Second, reaction 6 will allow the isomerization reaction $H^{18}O^{16}O \leftrightarrow H^{16}O^{18}O$ to occur and, through reaction with ozone, formation of $H^{16}O$, which is expected by experimentalists to be formed only via hydrogen abstraction. These two reasons question not only the mechanistic interpretation given by experimentalists but also the barrier height for hydrogen abstraction that is considered to be 1 ± 0.4 kcal mol^{-1} higher than the barrier for hydrogen abstraction.

Extrapolation of the coupled-cluster energies to the CBS limit was achieved through the USTE method. The improvements on the results are seen on the slight increase of ΔE^{iso}, which is negative when the double-ζ basis sets are used, and becomes positive with the increase of the cardinal number X.

Overall, the CASPT2 method was revealed to be the only one with an accurate description of both dynamical and nondynamical correlation effects in the structures calculated in this work. As for the DFT results, the BH&HLYP functional performed a little worse than all methods in the single-reference regions of the PES (excluding the CASSCF results) and better than the coupled-cluster methods in the multireference regions of the PES. However, this functional did not achieve the quality of the CASPT2 results in the latter regions of $HO_5(^2A)$.

We hope that the present theoretical work contributes significantly to the understanding of the title reaction for both experimentalists and theoreticians. It would be interesting to extend it with a study of the effect of quadruply excited clusters in the calculations of coupled-cluster energies of the geometries with a high degree of single-reference character and also of **SP$_1$**, which has still a considerable amount of single-reference character (65%). Furthermore, it would be interesting to thoroughly test different density functionals to compare the results with the CASPT2 energies obtained in this paper, since the use of DFT theory is simpler and computationally more affordable than MRPT, thus allowing

a more extensive mapping of the PES. Such developments will be part of a planned improvement of the DMBE $HO_5(^2A)$ PES on which further dynamics studies will be carried out.

Acknowledgment. The authors acknowledge funding from Fundação para a Ciência e a Tecnologia, Portugal (contracts REEQ/128/QUI/2005 and SFRH/BPD/40807/2007).

Supporting Information Available: Coordinates, frequencies, and absolute energies for all computed structures. This material is available free of charge via the Internet at http://pubs.acs.org.

References

(1) Monks, P. S. *Chem. Soc. Rev.* **2005**, *34*, 376–395.

(2) Wennberg, P. O.; Cohen, R. C.; Stimpfle, R. M.; Koplow, J. P.; Anderson, J. G.; Salawitch, R. J.; Fahey, D. W.; Woodbridge, E. L.; Keim, E. R.; Gao, R. S.; Webster, C. R.; May, R. D.; Toohey, D. W.; Avallone, L. M.; Proffitt, M. H.; Loewenstein, M.; Podolske, J. R.; Chan, K. R.; Wofsy, S. C. *Science* **1994**, *266*, 398–404.

(3) Duewer, W. H.; Wuebbles, D. J.; Ellsaesser, H. W.; Chang, J. S. *J. Geophys. Res.* **1977**, *82*, 935–942.

(4) Crutzen, P. J.; Howard, C. J. *Pure Appl. Geophys.* **1978**, *116*, 497–510.

(5) Whitten, R. C.; Borucki, W. J.; Capone, L. A.; Turco, R. P. *Nature* **1978**, *275*, 523–524.

(6) Turco, R. P.; Whitten, R. C.; Poppoff, I. G.; Capone, L. A. *Nature* **1978**, *276*, 805–807.

(7) Simonaitis, R.; Heicklen, J. *J. Phys. Chem.* **1973**, *77*, 1932–1935.

(8) DeMore, W. B.; Tschuikow-Roux, E. *J. Phys. Chem.* **1974**, *78*, 1447–1451.

(9) Zahniser, M. S.; Howard, C. J. *J. Chem. Phys.* **1980**, *73*, 1620–1626.

(10) Manzanares, E. R.; Soto, M.; Lee, L. C. *J. Chem. Phys.* **1986**, *85*, 5027–5034.

(11) Sinha, A.; Lovejoy, E. R.; Howard, C. J. *J. Chem. Phys.* **1987**, *87*, 2122–2128.

(12) Wang, X.; Soto, M.; Lee, L. C. *J. Chem. Phys.* **1988**, *88*, 896–899.

(13) Nelson, D. D.; Zahniser, M. S. *J. Phys. Chem.* **1994**, *98*, 2101–2104.

(14) Nizkorodov, S. A.; Harper, W. W.; Blackmon, B. W.; Nesbitt, D. J. *J. Phys. Chem. A* **2000**, *104*, 3964–3973.

(15) Herndon, S. C.; Villalta, P. W.; Nelson, D. D.; Wayne, J. T.; Zahniser, M. S. *J. Phys. Chem. A* **2001**, *105*, 1583–1591.

(16) Varandas, A. J. C.; Zhang, L. *Chem. Phys. Lett.* **2004**, *385*, 409–416.

(17) Mansergas, A.; Anglada, J. M. *J. Phys. Chem. A* **2007**, *111*, 976–981.

(18) Xu, Z. F.; Lin, M. C. *Chem. Phys. Lett.* **2007**, *440*, 12–18.

(19) Varandas, A. J. C. *Adv. Chem. Phys.* **1988**, *74*, 255–338.

(20) Varandas, A. J. C. In *Lecture Notes in Chemistry*; Laganá, A., Riganelli, A., Eds.; Springer: Berlin, 2000; Vol. 75, pp 33−56.

(21) Varandas, A. J. C. In *Conical Intersections: Electronic Structure, Dynamics & Spectroscopy*; Domcke, W., Yarkony, D. R., Köppel, H., Eds.; Advanced Series in Physical Chemistry; World Scientific Publishing: Singapore, 2004; Vol. 15, pp 205−270.

(22) Pople, J. A.; Head-Gordon, M.; Raghavachari, K. *J. Chem. Phys.* **1987**, *87*, 5968–5975.

(23) Boys, S. F.; Bernardi, F. *Mol. Phys.* **1970**, *19*, 553–566.

(24) Hansen, J. C.; Francisco, J. S. *ChemPhysChem* **2002**, *3*, 833–840.

(25) Mebel, A. M.; Morokuma, K.; Lin, M. C. *J. Chem. Phys.* **1995**, *103*, 7414–7421.

(26) Schmidt, M. W.; Baldridge, K. K.; Boats, J. A.; Elbert, S. T.; Gorgon, M. S.; Jensen, J. H.; Koseki, S.; Matsunaga, N.; Nguyen, K. A.; Su, S.; Windus, T. L.; Dupuis, M.; Montgomery, J., Jr. *J. Comput. Chem.* **1993**, *14*, 1347–1363.

(27) Werner, H.-J.; Knowles, P. J.; Lindh, R.; Manby, F. R.; Schütz, M. Molpro, a package of ab initio programs, version 2008.1; see http://www.molpro.net.

(28) Bode, B. M.; Gordon, M. S. *J. Mol. Graphics Modell.* **1998**, *16*, 133–138.

(29) Pulay, P.; Hamilton, T. P. *J. Chem. Phys.* **1988**, *88*, 4926–4933.

(30) Rode, M. F.; Werner, H.-J. *Theor. Chem. Acc.* **2005**, *114*, 309–317.

(31) Cramer, C. J.; Włoch, M.; Piecuch, P.; Puzzarini, C.; Gagliardi, L. *J. Phys. Chem. A* **2006**, *110*, 1991–2004.

(32) Cramer, C. J.; Kinal, A.; Włoch, M.; Piecuch, P.; Gagliardi, L. *J. Phys. Chem. A* **2006**, *110*, 11557–11568.

(33) Roos, B. O.; Taylor, P. R.; Siegbahn, P. E. M. *Chem. Phys.* **1980**, *48*, 157–173.

(34) Ruedenberg, K.; Schmidt, M. W.; Gilbert, M. M.; Elbert, S. T. *Chem. Phys. Lett.* **1982**, *71*, 41–49.

(35) Roos, B. O.; Linse, P.; Siegbahn, P. E. M.; Blomberg, M. R. A. *Chem. Phys.* **1982**, *66*, 197–207.

(36) Werner, H.-J.; Knowles, P. J. *J. Chem. Phys.* **1985**, *82*, 5053–5063.

(37) Knowles, P. J.; Werner, H.-J. *Chem. Phys. Lett.* **1985**, *115*, 259–267.

(38) Wolinski, K.; Sellers, H. L.; Pulay, P. *Chem. Phys. Lett.* **1987**, *140*, 225–231.

(39) Wolinski, K.; Pulay, P. *J. Chem. Phys.* **1989**, *90*, 3647–3659.

(40) Werner, H.-J. *Mol. Phys.* **1996**, *89*, 645–661.

(41) Celani, P.; Werner, H.-J. *J. Chem. Phys.* **2000**, *112*, 5546–5557.

(42) Purvis, G. D.; Bartlett, R. J. *J. Chem. Phys.* **1982**, *76*, 1910–1918.

(43) Knowles, P. J.; Hampel, C.; Werner, H.-J. *J. Chem. Phys.* **1993**, *99*, 5219–5227.

(44) Knowles, P. J.; Hampel, C.; Werner, H.-J. *J. Chem. Phys.* **2000**, *112*, 3106–3107.

(45) Raghavachari, K.; Trucks, G. W.; Pople, J. A.; Head-Gordon, M. *Chem. Phys. Lett.* **1989**, *157*, 479–483.

(46) Watts, J. D.; Gauss, J.; Bartlett, R. J. *J. Chem. Phys.* **1993**, *98*, 8718–8733.

(47) Dunning, T. H. *J. Chem. Phys.* **1989**, *90*, 1007–1023.

(48) Kendall, R. A.; Dunning, T., Jr.; Harrison, R. J. *J. Chem. Phys.* **1992**, *96*, 6769–6806.

(49) Woon, D. E.; Dunning, T. H., Jr. *J. Chem. Phys.* **1995**, *103*, 4572–4585.

(50) Helgaker, T.; Klopper, W.; Koch, H.; Noga, J. *J. Chem. Phys.* **1997**, *106*, 9639–9646.

(51) Halkier, A.; Helgaker, T.; Jørgensen, P.; Klopper, W.; Koch, H.; Olson, J.; Wilson, A. K. *Chem. Phys. Lett.* **1998**, *286*, 243–252.

(52) Truhlar, D. G. *Chem. Phys. Lett.* **1998**, *294*, 45–48.

(53) Halkier, A.; Helgaker, T.; Jørgensen, P.; Klopper, W.; Olsen, J. *Chem. Phys. Lett.* **1999**, *302*, 437–446.

(54) Varandas, A. J. C. *J. Chem. Phys.* **2000**, *113*, 8880–8887.

(55) Karton, A.; Martin, J. M. L. *Theor. Chim. Acta* **2006**, *115*, 330–333.

(56) Varandas, A. J. C. *J. Chem. Phys.* **2007**, *126*, 244105.

(57) Yu, H. G.; Varandas, A. J. C. *Chem. Phys. Lett.* **2001**, *334*, 173–178.

(58) Varandas, A. J. C. *ChemPhysChem* **2005**, *6*, 453–465.

(59) Varandas, A. J. C.; Zhang, L. *Chem. Phys. Lett.* **2000**, *331*, 474–482.

(60) Mansergas, A.; Anglada, J. M. *ChemPhysChem* **2007**, *8*, 1534–1539.

(61) Mathisen, K. B.; Siegbahn, P. E. M. *Chem. Phys.* **1984**, *90*, 225–230.

(62) Chen, M. M. L.; Wetmore, R. W.; Schaefer, H. F., III *J. Chem. Phys.* **1981**, *74*, 2938–2944.

(63) Dupuis, M.; Fitzgerald, G.; Hammond, B.; Lester, W. A., Jr.; Schaefer, H. F., III *J. Chem. Phys.* **1986**, *84*, 2691–2697.

(64) Varandas, A. J. C. *Theor. Chem. Acc.* **2008**, *119*, 511–521.

(65) Lee, T. J.; Taylor, P. R. *Int. J. Quant. Chem. Symp.* **1989**, *23*, 199–207.

(66) Leininger, M. L.; Nielsen, I. M. B.; Crawford, T. D.; Janssen, C. L. *Chem. Phys. Lett.* **2000**, *328*, 431–436.

(67) Lee, T. J. *Chem. Phys. Lett.* **2003**, *372*, 362–367.

(68) Piecuch, P.; Kucharski, S. A.; Kowalski, K.; Musial, M. *Comput. Phys. Commun.* **2002**, *149*, 71–96.

(69) Piecuch, P.; Włoch, M. *J. Chem. Phys.* **2005**, *123*, 224105.

(70) Piecuch, P.; Włoch, M.; Varandas, A. J. C. In *Topics in the Theory of Chemical and Physical Systems*; Lahmar, S., Maruani, J., Wilson, S., Delgado-Barrio, G., Eds.; Progress in Theoretical Chemistry and Physics; Springer: Dordrecht, The Nederlands, 2007; Vol. 16, pp 63−121.

(71) Varandas, A. J. C. *ChemPhysChem* **2002**, *3*, 433–441.

(72) Zhang, L.; Varandas, A. J. C. *Phys. Chem. Chem. Phys.* **2001**, *3*, 1439–1445.

CT900370Q